(2)

4. **REMOTE SENSING**

METRIC PROPERTIES OF IMAGERY PRODUCED BY SIDE-LOOKING AIRBORNE RADAR AND INFRARED LINESCAN SYSTEMS

by

Dipl. Ing. F. Leberl

1. Introduction

This report deals with the geometric analysis of two typical kinds of photographic record with which the photogrammetrist will increasingly become confronted: those produced by Side-Looking Airborne Radar (SLAR) and Infrared Line Scan (IRLS) systems.

Military security restrictions are being relaxed, thus releasing more and more of the hardware connected with these new imaging systems; at the same time civilian science is continuously developing other data gathering methods [5] .
The problem arises of how to correlate the information from different sources and how to reduce it to a usable form. The pertinent geometric problems should be investigated by photogrammetrists.

Towards this end, a number of efforts have been reported in literature, mainly concerned with IRLS [7] and SLAR [19] , but also with various non-imaging remote-sensing systems [4] . The use of unconventional imaging systems does not have to be limited to the gathering of qualitative (or non-metric) information, but can be extended to the extraction of quantitative (or metric) information too, in which case the additional tool becomes a "tool in itself" [11] . This has not yet been proven completely, but the successful construction of topographic maps from SLAR-imagery, reported in [3] , while still depending on the extensive use of auxiliary data, has shown the direction of development.

Thus a new generation of "grammetric" principles will enrich the field of photogrammetry. In order to estimate the value and limitations of these principles, the geometric performance of SLAR- and IRLS-systems is investigated in this report.

These two systems may be considered to be those of most interest to the photogrammetric community and incorporate features typical of other current remote-sensing systems. The geometric reliability of the imagery generated by these systems is still far inferior to that of the aerial camera. Nevertheless this imagery has potentials, which, under certain circumstances, make it a useful replacement for or supplement to conventional photography.
Examples might include the well-known all-weather capability of radar and its possibility of synoptic views, or the fact that IRLS-imagery is a record of variations in emissivity from the object area rather than of variations in reflectivity as in photography. This latter example allows e.g. the mapping of an ice-covered shore-line, since the thermal emission from the ice on the sea differs from that resting on the land. No such difference can be detected in the reflected visible radiation as measured by photography.

Further discussions of these possible applications goes beyond the scope of this report. In the following paragraphs, therefore, first the equipment of the SLAR- and IRLS-systems will be described, including considerations of resolution, scale and micro-performance of the photographic records (pointing accuracy). Next the macro-performance (image displacements) of the imagery will be analysed. and the results presented in graphical form. Subsequently some discussion follows about planimetric plotting and contouring from SLAR- and IRLS-records.

2. Image Formation

Most of the new types of imagery are formed by scanning the object-space line by line and even point by point from an air- or spacecraft, and recording on film the intensity of the sensed electromagnetic radiation after its transformation into a video-signal.
As this does not happen instantaneously for a whole film strip, the records are affected by any change of the system, and so are said to be "dynamic". The whole image producing system or often only its sensing component is referred to as a "sensor".

2.1 Side-Looking Airborne Radar (SLAR)

Basically, there are two quite different systems: real- and synthetic aperture SLAR. The latter appears to have more potential for mapping purposes but it is not yet available for civilian use due to its military classification. Real aperture SLAR is commercially available [13] and therefore will be discussed here. The hardware of a real-aperture SLAR costs about $ 100,000, or a synthetic-aperture SLAR about $ 250,000 [0].

Commercial offers of SLAR-mosaics, together with the pertinent interpretation at a scale of 1:250,000 have been made at a cost of about $ 10 per square mile. SLAR coverage of an area of 52,000 sq. km now being undertaken for the purpose of oil exploration will cost about $ 250,000 [2] .

2.1.1 Principle

Real-aperture SLAR is an active (i.e. with its own source of illumination), line-scanning system which measures echotime.
In the imagery, the x-axis of the coordinate-system is defined to lie in the direction of flight and the y-axis cross-track. The conjugate coordinates on the ground are X and Y. The imagery is formed in the following way (fig. 1 a):

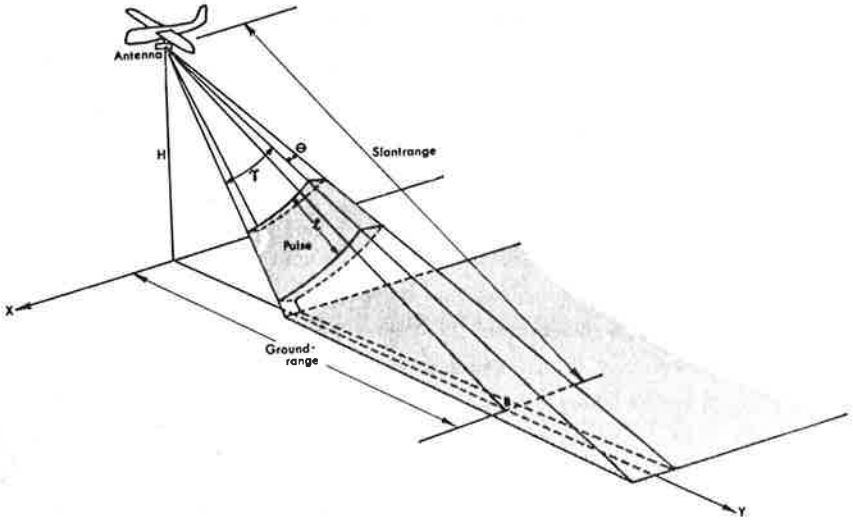

Fig. 1a. Geometrical characteristics of the SLAR system in the object space.

A long antenna is fixed to the body of the aircraft, parallel to its longitudinal axis, and emits pulses of electro-magnetic radiation of a specific wavelength, in most cases between 0.5 and 8 cm.
The pulses are propagated in a fan which lies approximately in a plane perpendicular to the longitudinal axis of the aircraft and has a limited angular width γ in that plane. The radiation is reflected from the ground.
A fixed period after each pulse is emitted, the electron-beam of a cathode

ray tube (CRT) starts sweeping across the screen in the y-direction. The reflected signals from the ground are detected by the antenna, transformed into electric signals and used to modulate the intensity of the electron-beam, which, after reaching the edge of the CRT screen, returns to its zero-position. The next pulse can then be transmitted.

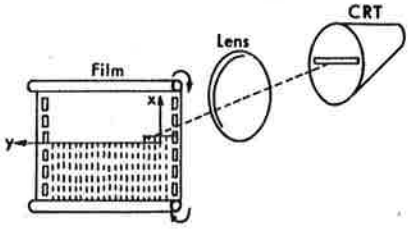

Fig. 1b. Image recording with SLAR.

The image on the CRT is recorded on film (fig. 1b). The scanning of the object area in the X-direction is performed by the forward movement of the aircraft and the filmtransport, so that a strip of the object area is imaged line by line. If the velocity of the electron-beam across the screen is proportional to the speed of the electromagnetic pulses in the air, then the y-coordinates represent distances between the antenna and the object, the so-called "Slant-ranges". Since the above described procedure repeats itself at a rate of thousands of cycles/second (for example 2100 c/sec. in the Westinghouse-system) the record on film is similar in appearance to an aerial photograph, and does not represent a discrete composition of lines. Thus every object is, and indeed must be illuminated many times and the lines are integrated to form a continuous image.

2.1.1 Geometric Resolution

At a certain moment of time, a SLAR-system detects the average intensity of the reflection of the emitted signal from a finite area, called "ground-resolution element". In an optimized system, this basically defines the resolution of the final photographic record.

The resolutions in the X- and Y-directions (on the ground) are different. In the X-direction, it is called the "azimuthal resolution" since it depends on the azimuthal opening angle θ of the antenna beam (fig. 1a). In the Y-direction, it is named "range resolution" and depends on the length l of the emitted pulse.

Range-resolution: The signal received from a (point-) target lasts for a time interval $t_o = l/v$, where l is the spatial pulse length, and v the velocity of a pulse. s is the slant range to the target, so 2s/v is the time of travel of the radar pulse to the object and back ("round-trip time"). Radar echoes from two separated object-points, which arrive in a time interval defined by $2s/v \leq t \leq 2s/v+t_o$, are superimposed.

The round trip time $2s/v+t_o$ corresponds to a slant range s+d. d is defined from $2(s+d) = v\,(2s/v+t_o)$ as: $d = t_o v/2 = l/2$. So to completely resolve two adjacent targets, their minimum range difference must be half of the pulse length.

Resolution in azimuth: The pulses do not propagate in a plane, but in a conically shaped beam* of finite angular width θ, which is given by the formula $\theta = 1.2\,\lambda/D$, where D is the length of the antenna ("aperture size"), and λ the wave length of the radiation. At a slant range s, the azimuthal resolution amounts to $1.2\,\lambda\, s/D$ (fig. 2).

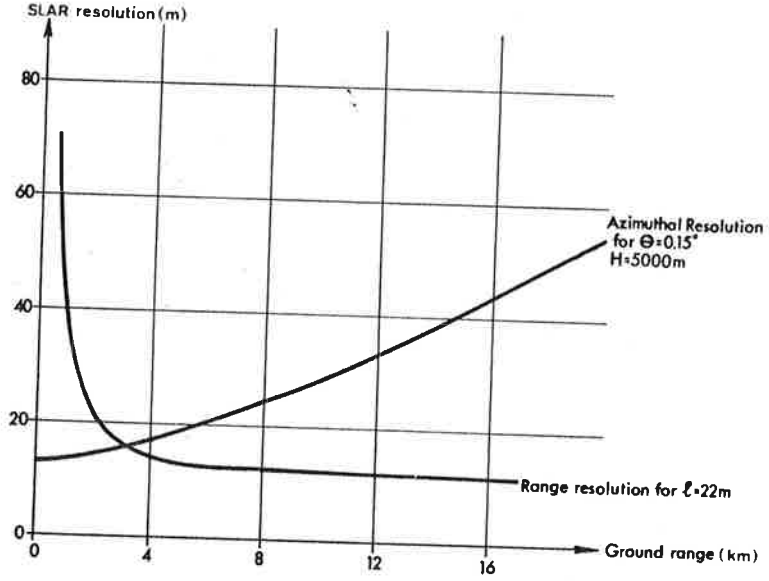

Fig. 2. Ground resolution of the SLAR system.

* The beam forms a cone whose vertex angle is near π. Throughout the paper, therefore, the conical shape is neglected and a plane beam assumed.

At short distances from the aircraft's ground track - i.e. at short "ground ranges" - the range resolution becomes very poor. This is the reason that the area below the aircraft, up to a ground range equal to half the flying height, is not imaged in the SLAR-record. Imagery taken at a depression angle of 75^{o} is sometimes still considered to be useful. A further conclusion from fig. 2 is, that at larger ranges the range resolution is far superior to the azimuthal one.

2.1.3 Micro-accuracy

The accuracy related to the measurement of image coordinates is referred to as "micro-accuracy". Experiments have been performed at the ITC to determine the accuracy with which signalized geodetic ground control points can be measured on a SLAR image.

The signalization of these points has been carried out using special corner reflectors with a surface about 10^{4} (in area) smaller than one ground resolution element. The reflectors - though dimensionally too small to be visible - raise the average intensity of the reflected signal to such an extent, that they become visible (fig. 3a). Although this is possible in conventional photography too, it is far less important there than in SLAR.

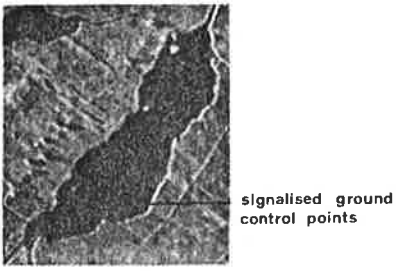

Fig. 3a. Detail of the SLAR-imagery with corner reflectors.

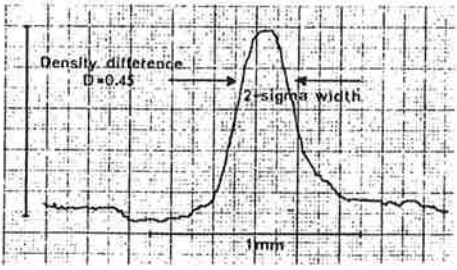

Fig. 3b. Density trace of the spread signal from a corner reflector.

Based on the assumption that a compatible measuring mark is chosen, the mean pointing error has been estimated by Hempenius [6] to be about 5% of the '2-sigma' -width of the observed photographic signal.

Measurements on the imagery of fig. 3 using a monocomparator have shown that the standard deviation in pointing to the spread signal from a point source is $\pm$ 10 μm at a scale of 1:200.000. For the purpose of comparing these figures with the theoretical estimate of Hempenius, the

density profiles across some of the most characteristic reflector images have been measured by a micro-densitometer.
The density trace (fig. 3b) has been transformed into an intensity profile and the 2-sigma width of the signal determined from the nomograms given in [6] .
The spread signal from the corner reflectors was found to be about 200 μm. This blur or unsharpness is caused by the limited imaging quality of the complete SLAR equipment. This quality is about equal in x and y (circular symmetry in the blurred point images). 5% of 200 μm is 10 μm, so the experimentally obtained value of the pointing error matches the predicted one. This means that the ultimate accuracy of well selected signalized points (preferably corner reflectors on water) will be of this order (± 10 μm) for the current real-aperture SLAR.

2.1.4 Scale

Since the scale of a SLAR-image changes along the y-axis due to the "slant-range"-projection, only an average scale number can be defined. This is the width of the imaged ground strip divided by the width of its record on film. Another scale number can be produced by considering the factor by which the velocity of the CRT-spot is reduced compared to half the speed of the pulse in the air.

For the first method, the film width may be determined in the following way:
The projection of one CRT y-line on the ground consists of a certain number of ground resolution elements. This number should not exceed the number of resolution elements of the CRT. The resolution of the film should also match these requirements. A typical high quality CRT contains 6000 points* in a line of 10 cm length, which corresponds to a resolution of 30 lines/mm [13]. Films have to be 10 cm wide if there is no enlargement between CRT and

* This CRT-resolution is superior for present civilian SLAR systems (compare, for example, with the number of ground resolution elements in one Y-line). It can only present a bottleneck in the case of systems with extreme resolution.

film and they should resolve 40 lines/mm. Thus, well designed SLAR-systems will record the signals from a slant range width of 8 km at a scale of 100.000, or 15 km at 1:200.000. For civilian purposes, the width of the terrain strips which are imaged are usually not more than 15 to 20 km, because the image-quality deteriorates for wider ranges. However, for special purposes, SLAR-widths of up to 50 km have been achieved [13], and this certainly does not represent a limit to the state of the art.

2.1.5 Future development

It has been shown that the ground resolution in X-direction of real-aperture SLAR is the bottleneck in the system as it is inferior to the range resolution. Synthetic-aperture SLAR has an improved resolution in azimuth. In this system the reflected radar signals together with a coherent reference wave, are used to generate interference patterns, as in optical holography. The resulting record on film is therefore a microwavehologram, which can only be transformed into an image of photographic appearance by complex processing [18]. Its azimuthal resolution depends on the processing of the holograms. The theoretical optimum is given by Revillon [18] as $(\lambda . s/2)^{\frac{1}{2}}$ or D/2 respectively for the two methods of processing. Another development which can be expected in the near future is that the signals will be stored on magnetic tape, metallic foils or crystals [13] so that the recording need no longer be made exclusively on a CRT or on film.

2.2 The Infrared Line Scanner

An IRLS-system is comparatively cheap - about the same as an aerial camera [1]. In the near future, one may expect many of these systems to be used operationally for the purpose of gathering quantitative (i.e. non-metric) information.

2.2.1 Principle

The IRLS-system is a passive line scanner - passive in the sense of having no internal source of illuminating the terrain. A rotating prism with one or more faces receives the electro-magnetic radiation emitted from a resolution patch on the ground (fig. 4a).

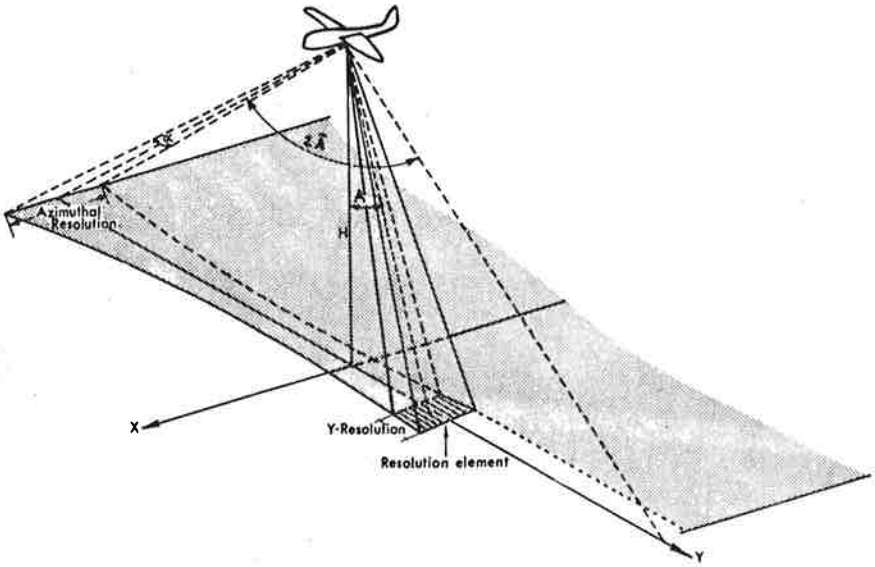

Fig. 4a. Geometrical characteristics of the IRLS system.

The radiation is projected via a parabolic mirror onto a detector which transforms a specific wavelength between 1 μm - 15 μm into an electric signal.

This signal may be recorded in one of three ways.

In the first case, the recording system uses a CRT-spot and is quite similar to that employed with the SLAR; in the second case the signal modulates the intensity of a glowlamp and its light is projected via an optical system onto film (fig. 4b).

The third way is to record the signal on a magnetic tape (which is used later to modulate a CRT-spot or a glowlamp to produce an image).

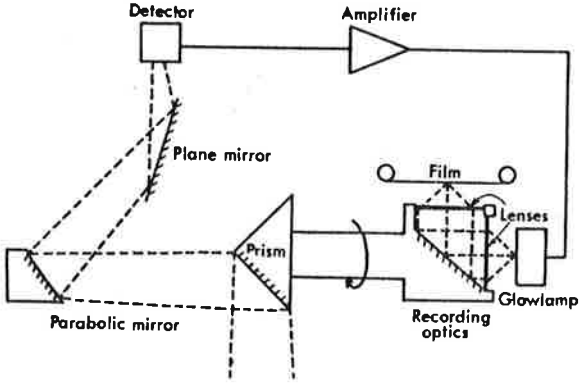

Fig. 4b. Image sensing and recording system of IRLS.

Scanning in the x-direction is again accomplished by the movement of the aircraft and film. Scanning in the y-direction is achieved by rotating both the prism and the recording optical system around the same axis at a constant speed of 6000 cycles/min.
An increase of that speed to about 12000 c/min. is considered to be feasible at present [12] .

If the received radiation is split into its component wavelength bands, the intensity of each band being transformed into a video-signal and stored separately, one speaks of "Multi-Spectral - Sensing" (MSS). This kind of recording may allow "pattern recognition" (automatic interpretation of the data) to be carried out.

2.2.2 Resolution

The resolution of the IRLS-system is determined basically by the instantaneous angle of view α (fig. 4a) of the scanning optics consisting of prism and parabolic mirror. In current civilian scanners this angle amounts to 1.5 - 2.5 milliradians [1] .
The size of the ground resolution element is also a function of the flying height and scan angle A. Figure 5 shows the relation graphically.

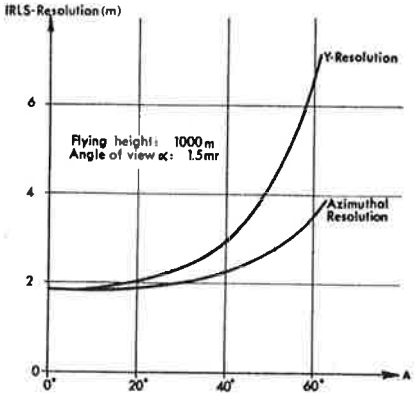

Fig. 5. Ground resolution of IRLS.

2.2.3 Scale

The y-coordinate on the imagery is proportional to the angle that the line of sight from the sensor to the target forms with the vertical. Thus there are large scale changes due to the panoramic scanning method.
Both the scale number and the size of a ground resolution patch are variable.

S_1 is the scale number for targets on the flight path and S_2 an average scale number, which is the width of the imaged ground strip divided by the width of its photographic record. As for SLAR, the scale has to be such that all resolution patches, especially the smallest directly below the aircraft, are resolved on film.

The maximum permissible scale numbers S_1, S_2 result therefore from the formulae

$$S_1 = H/f \qquad \text{and} \qquad S_2 = S_1 \cdot \tan(\bar{A}) \; / \; \bar{A}$$

where f is defined as $f = 1/(\alpha \cdot n)$ and represents an equivalent focal length (n is the film resolution in lines/mm, H the flying height and $\bar{A}$ half of the total angular coverage of the system (fig. 6)).

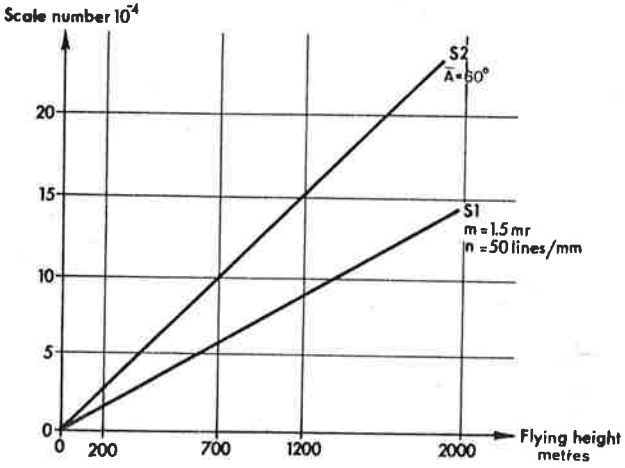

Fig. 6. Scale of IRLS imagery

3. Image displacements

Every deviation of the geometrical properties of SLAR - and IRLS-imagery from the cylindrical equidistant projection of the object area - with the standard parallel being a great circle along the track of the aircraft on the earth's surface - is considered to be an "image-displacement".

The sources of displacement can be classified in three groups, namely

- geometry of the projection ("viewing geometry") and topography
- exterior orientation
- interior orientation

The image displacements as given in this analysis are expressed in metres in the terrain as the whole approach has been based on the idea of using

the imagery as a map substitute. The coordinate system is given in fig. 7.

Fig. 7. Coordinate system.

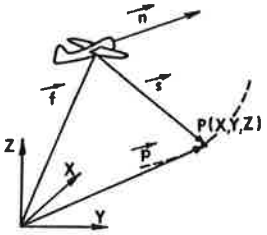

Fig. 8. Vectorial representation.

However for numerical evaluation of overlapping imagery a completely different approach is to consider the image coordinates only as an intermediate source of information which relates the image to eventual records of the exterior and interior orientation. In vectorial representation, this would be formulated as (fig. 8):

$$\vec{f} + \vec{s} = \vec{p}$$
$$\vec{s} * \vec{n} = o$$

In any kind of strip imagery, the x-coordinate relates the image point to the vectors $\vec{f}$ and $\vec{n}$ (position and attitude of the platform) and the y-coordinate to the vector $\vec{s}$.

3.1 SLAR-system

The x-coordinate of an image point on a SLAR film-strip gives the time the conjugate object point has been imaged. The y-coordinate can have two different meanings. First, there is "slant range" presentation, in which $y = (v.t/2 - v.\frac{e}{2})k$, where t is the round trip time, v the velocity of the pulse, e a constant value, called "sweep delay", and k a scale factor.

Secondly there is "ground range" presentation, in which $y = (((v.t/2)^2 - H^2)^{\frac{1}{2}} - (v^2.e^2/4 - H^2)^{\frac{1}{2}})k$, where H is the height of the platform. The ground range presentation is achieved by a non-linear sweep of the electron-beam across the CRT.

3.1.1 Geometry of the Projection

A formula for the image displacement Δy due to the viewing geometry and topography has been derived with the assumption that the minimum ground range, at which recording begins, is of the size of the flying height.

This formula includes the effect of ground height differences and earth curvature, (fig. 12):

$$k.\Delta y = (s-G_o) + (\Delta h^2 - 2H.\Delta h)/2G_o + HG_o/2R + (2G_o^2 - (H+\Delta h)(\Delta h-2H).$$

$$\Delta h)/4.G_oR$$

$$k.\Delta x = o$$

(for the derivation see Appendix)

where s is the measured slant range, $G_o = (s^2 - H^2)^{\frac{1}{2}}$, H is the flying height, Δh the height of the object above the datum surface, R the radius of the earth and k a scale factor.

Figure 9 shows the effect of the first term, i.e. of the slant range presentation.

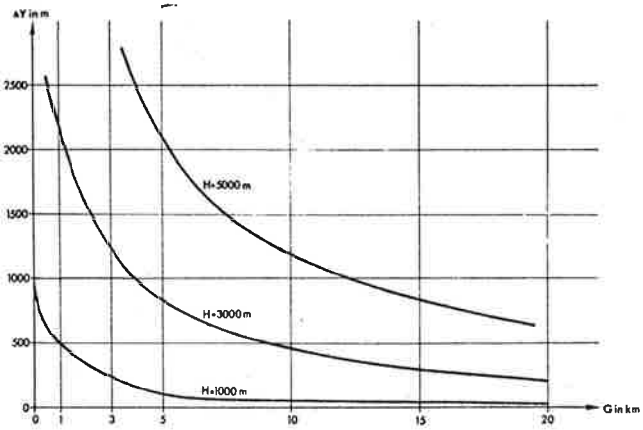

Fig. 9. Image displacement due to "Slant Range Presentation" in SLAR.

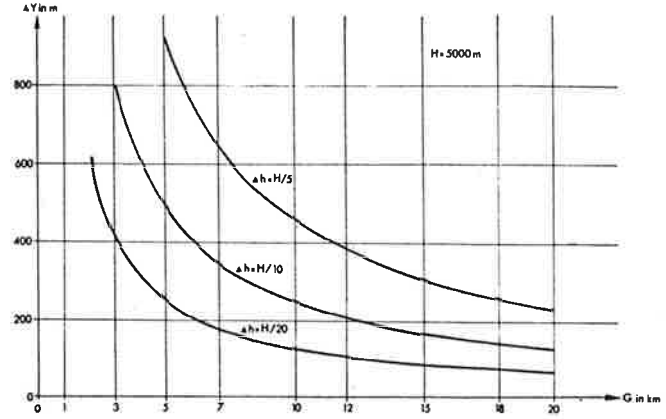

Fig. 10. Image displacement due to ground height differences Δh in Slar.

Even under extreme conditions, with H = 10 km, Δh = 2.5 km, the 4th term can only be about 1 m. As the effect of earth curvature (the 3rd term) does not exceed 10 m under operational conditions, it does not need to be considered as far as available equipment is concerned.

Height differences on the ground provide an additional displacement of $(\Delta h^2 - 2\,\Delta hH)/2G_o$. (See fig. 10). For smaller values of $\Delta h/G_o$, this reduces to $-\Delta hH/G_o$. The "relief displacement" is directed radially towards the nadir of the sensor. Therefore the images of slopes that are inclined towards the aircraft, are compressed, especially for smaller values of G_o. This can limit the width of the SLAR-strip which can be used for interpretation purposes.

3.1.2 Exterior Orientation

The sensor changes its exterior orientation continuously. Its position is determined by its speed and height, the heading (the angle between the aircraft's longitudinal axis and the north direction), the drift-angle (between the aircraft's longitudinal axis and the direction of forward movement) and time. The angular orientation of the sensor is given by the yaw or swing (κ), pitch or tip (φ) and roll or tilt (ω).* Continuous recordings of the orientation parameters show that the sensor deviates from the ideal flight path and attitude in a periodic manner. The frequency and amplitude of the deviations depend on the type of aircraft and the environmental circumstances [17] . This has to be studied in order to estimate the relative accuracy of the imagery and efforts in this direction are under way in the ITC.

The sensor deviates from its ideal position due to changes of speed, height, heading and drift-angle. Attitude changes affect the orientation of the antenna beam due to variations in yaw or swing ($d\kappa$) and pitch or tip ($d\varphi$). A change of roll or tilt ($d\omega$) does not result in a geometric error as it does not change the distance between sensor and object or the time of illumination.

* In remote-sensing literature, the navigational terms yaw, pitch and roll are used in place of the photogrammetric swing, tip and tilt.

The image displacement due to an erroneous exterior orientation can be formulated as:

$$k.\,\Delta y = -\,(G_o/s)\,dby + (H/s)\,dbz + (G_o^{\,2}/2s)\,d\kappa^{\,2}$$

$$k.\,\Delta x = G_o\,d\kappa - dbx + Hd\varphi \qquad \text{(for derivation see Appendix)}$$

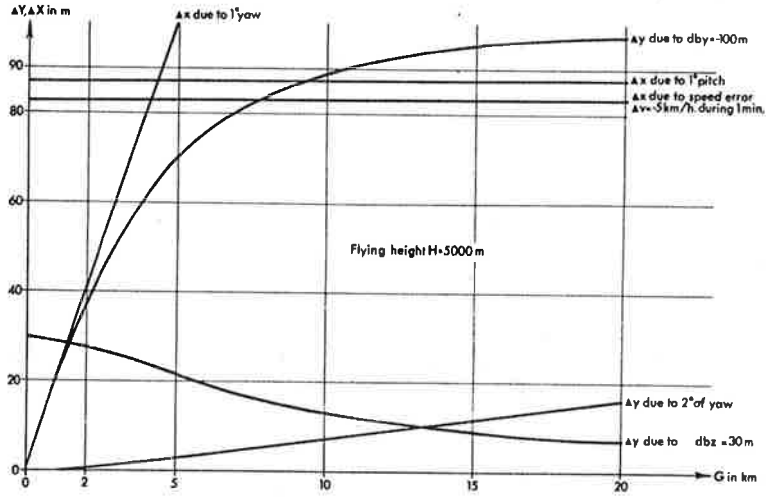

Fig. 11. Image displacements due to errors in exterior orientation in SLAR *

where dbx, dby and dbz are the deviations of the actual from the ideal flight path. The dbx is caused by an erroneous synchronization of the film and platform-speed and results from the formula dbx = (X/V)dV, where V is the speed of the platform and dV its error. The systematic component of dV gives a systematic scale change in x.
However the systematic components of these errors are not as crucial as their random parts. This is especially true for the effect of the yaw or swing κ . The rather large, constant component due to the drift angle, that is usually present as a result of wind conditions results - if no compensation is provided - only in a constant shear-deformation of the

* The second order effect of dk is considered here because of the comparatively large k values feasible.

image, whereas the small continuous changes of the heading (the variation in yaw or swing $d\kappa$) cause most disturbing image displacements, double mapping and gaps in the coverage. Thus, stabilization of the sensor is obviously of considerable importance in SLAR.

3.1.3 Inner Orientation

The geometric relation between the measured entities in the object space and their corresponding analogues on the photographic record is given by the inner orientation.

The display and recording units are subject to random and systematic perturbations, causing the inner orientation to be erroneous. As far as the electronic sweep is concerned, empirical studies have shown that the maximum error does not exceed 0.5 - 1% of the length of the sweep [16]. The errors are composed of non-linearities of the speed of the spot, erroneous orientation and the effects of curvature of the CRT-screen.

The recording unit, lens and film (fig. 1b) can only be adjusted with a limited accuracy, so that

- the direction of the film movement may not be perpendicular to the sweep on the CRT
- the recording lens can have an erroneous principal distance
- the film plane may not be parallel to the sweep on the CRT.

The errors in an individual recording system are systematic but must be determined separately for each set in use.

Refraction: Usually a SLAR film strip shows range marks for measuring slant or ground range. The relation between the actual speed of the electro-magnetic pulse in the air and the speed of the electronic spot on the CRT has to be established accurately.
It is a function of the refractive index r of the atmosphere, so that an error dr of the refractive index causes an error ds in the measured slant range:

$ds = -s\, dr/r$

As $dr < 3.10^{-4}$, $s < 2.10^{4}$ metres and $r > 1$, so ds is always smaller than 6 m, showing that this error is negligible. In this connection, it is evident that the curvature of the ray path due to changing refractive index does not affect the measured distance or the line of sight significantly.

3.2 IRLS-system

3.2.1 Geometry of the Projection

As y is determined from y = A.f, large image displacements in the y-direction are to be expected. The relation between the central perspective, the cylindrical projection and the IRLS geometry is shown in fig. 12. The discrepancies between the imagery and the cylindrical reference projection are, neglecting terms of 2nd and higher order:

$$k.\Delta y = H(A-\tan A) + \Delta h.\tan A - \frac{\tan^3 A.H^2}{2R} + \tan A\,\frac{\Delta h}{R}\,(H-\Delta h + \frac{\tan^2 A}{2}\,(2H-\Delta h))$$

$$k.\Delta x = o$$ (for derivation see Appendix)

where A is the angle between the line of sight to the object and the vertical (see fig. 13).

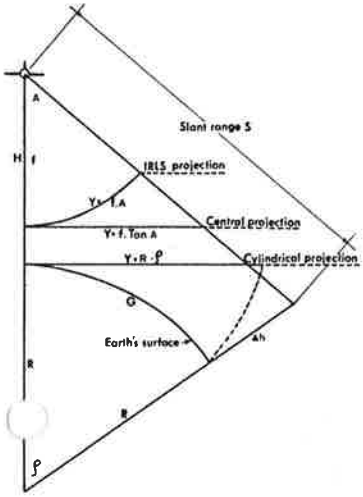

Fig. 12. Relationship between projections.

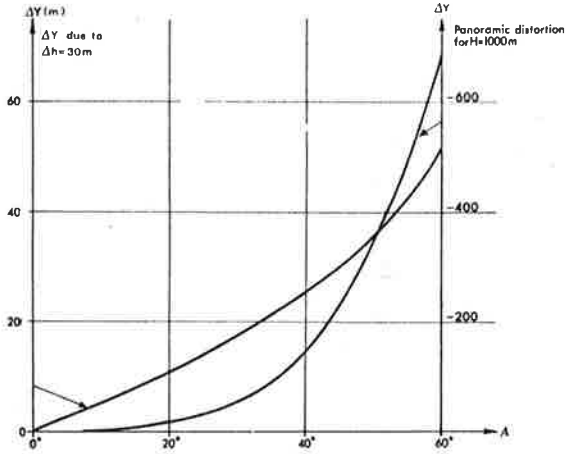

Fig. 13. Image displacements due to height differences and scanning method.

For $\Delta h=o$, $R \longrightarrow \infty$, the formula simplifies to that found in [7] : $\Delta y = H(A-\tan A)$. The earth can again be assumed to be flat, since the 3rd and the 4th terms, under operational conditions (i.e. H=2 km, $A=60^o$, $\Delta h=0,25H$), are smaller than 1 m.

3.2.2 Exterior Orientation

The IRLS records are more sensitive to changes in the exterior orientation than SLAR as their resolution on the ground is greater and their scale $1:S_1$ usually much larger. In addition, roll or tilt (ω) becomes a very significant source of image displacements. They result from the formula:

$$k.\Delta y = -\cos^2 A.\,dby - \sin 2A.\,dbz/2 + ((H.\sin 2A)/4)d\kappa^2 - H.\,d\omega$$

$$k.\Delta x = \tan A.\,H.\,d\kappa - dbx + H.\,d\varphi$$

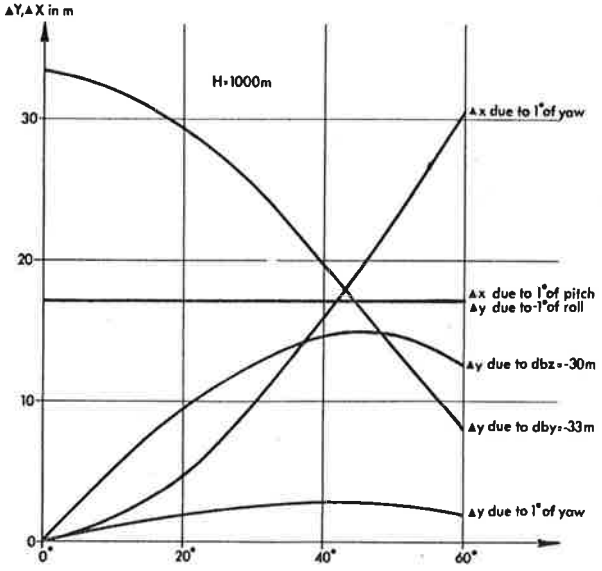

Fig. 14. Image displacements due to errors in exterior orientation.

The increased sensitivity of IRLS to changes of the exterior orientation results in a still more stringent requirement for stabilization than in SLAR.

3.2.3 Inner Orientation

If the recording is made from a CRT, then the arguments of section 3.1.3 also apply here. When a rotating optical system and a curved film are employed, the sources of distortion are described as follows [7] :

- misalignment of the scanning prism and recording optics, resulting in an error of the scan angle (which acts in the same manner as a roll or tilt)
- x- and y-axes of the film being non-perpendicular to the axis of the recording optics
- the film not moving perpendicular to the scanning direction.

Electronic time delays, lens distortion, erroneous focal length and non-verticality of the plane in which the optical axis of the scanner moves, have similar effects as in the SLAR-system and can be calibrated.

4. Mapping from the Imagery

At present, imagery is used almost exclusively for non-metric purposes, using modern viewing instruments with anamorphic optical trains in order to carry out the visual interpretation. But methods are available which allow metric handling of the data.

4.1 Rectification of a Single Strip of Imagery

The principle of rectifying a single strip of imagery is the same as that of conventional photogrammetric rectification. The approach can be numerical or instrumental.

Numerical rectification will normally be applied to individual points and implies the measurement of image-coordinates and subsequent calculation of ground coordinates. This can be done with the help of ground control, and either with or without recorded flight-data and sensor parameters, using a transformation to be derived from the formulae of section 3.

The instrumental approach would provide a corrected photograph. Without continuous manual or automatic control of the instrument and the provision of the appropriate navigational and topographic data, only those displacements resulting from the viewing geometry could be eliminated. A discussion of various rectification principles is given in [10] . The conclusion from these studies has been that a universal rectifier for a variety of types of scan imagery could be fabricated without a large technological effort, using the well known principles of differential rectification.

4.2 Plotting from Overlapping Imagery

4.2.1 Overlapping Imagery

Overlapping SLAR-imagery, generally called "parallel-pass" imagery, can be obtained by flying parallel flight lines. The overlap can be on the same side of both flight tracks or in between them ("same side" and "opposite side" stereo*). Rosenfield [19] showed, that the latter is superior due to its more favourable error propagation. There is, however, also the possibility of producing "stereo-imagery" from a single platform by sending out electro-magnetic pulses alternately in slight forward and backward directions, in a manner analoguous to the photogrammetric systems of convergent photography. At present such a system is being investigated [15].

For IRLS-imagery, there are three methods for obtaining overlaps. Firstly, there is the use of parallel flight lines. Secondly, overlaps may be achieved by utilizing two prisms on two rotation axes, each set at small angles to the aircraft's longitudinal axis (fig. 15a). Finally, there may be two prisms on one rotation axis, but one looking slightly forward and the other backward (fig. 15b). The last solution, though giving an additional hyperbolic distortion in x-direction due to the viewing geometry, has the best error propagation for the determination of heights.

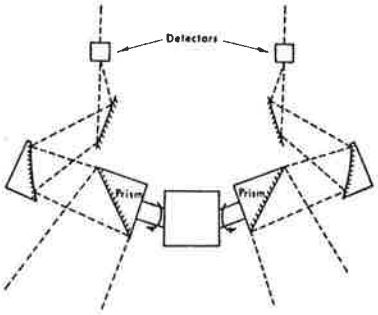

Fig. 15a.

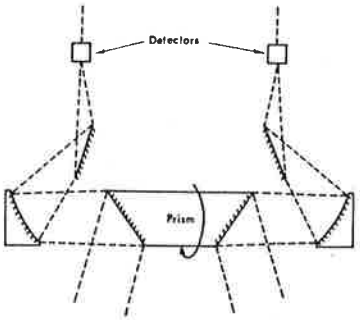

Fig. 15b.

Figs. 15. Vertical sections through IRLS sensor producing overlapping imagery.

* In remote-sensing literature, the photogrammetric meaning of "stereo" does not always apply. Often it is used to denote the use of overlapping imagery, which from the visual point of view may in fact be "non-stereo".

4.2.2 Plotting Methods

The purpose of producing overlapping imagery is generally the construction of contours. As stereovision is very difficult for SLAR and IRLS, the numerical approach seems to be the most suitable. Few workers have reported successful trials of stereovision with SLAR [8] , [9] .
Image coordinates, flight data and ground control would be used together for the calculation of the spatial ground coordinates of individual points. The measurement of flight data is expensive and not accurate enough for the construction of contours from parallel pass imagery. Thus for contouring from such imagery, the following approaches may be considered [20] :

i) Flight lines with a very large overlap are flown and APR spot heights are measured. Their planimetric locations are determined from navigation data or from the imagery itself since conventional photography may not be possible due to weather conditions. Additional heights may be interpolated from the imagery within the fairly dense net of APR heights.

ii) Another method for densifying the net of spot heights is by means of an interferometer, also called "3-dimensional" radar (fig. 16).

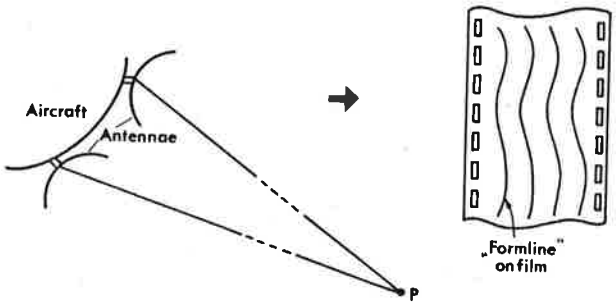

Fig. 16. "3-dimensional" radar - the interferometric method [14] .

One antenna, carried by the aircraft, transmits radar pulses, the reflections of which are sensed by this and another antenna. The two signals are brought together to form an interference pattern, which is continuously recorded during the flight. The resulting lines of constructive interference can be interpreted as form lines of the terrain. Further reduction of the data, using the SLAR-imagery and navigation data in addition to the interferometer patterns, provides contours. The possibilities from overlapping but simultaneously exposed IRLS-imagery will be discussed by Professor Konecny at this meeting.

5. Conclusions

The geometry of SLAR and IRLS imagery has been studied with respect to three error generators, namely viewing geometry, sensing equipment and sensor platform.

The most important distortions which have been found result from: the geometry of the projection, the yaw or swing of the sensor and the topography of the object area. Stabilization of the sensors reduces the errors resulting from an erronuous attitude. Although this does not produce the absolute location of the image points, stabilization is of great importance since it reduces the relative errors (e.g. due to yaw or swing). It is certainly superior to the bare recording of the attitude data with subsequent rectification, since the irreparable loss of information due to the double mapping and gaps is avoided. However, in order to compensate continuously for distortions resulting from other errors in exterior orientation, navigational data for the determination of the actual flight path of the sensing platform have to be recorded.

Planimetric rectification is most easily done instrumentally followed by mosaicing. Hardware has still to be developed for this purpose.

Contours can be obtained from overlapping imagery and this is one of the more interesting aspects of remore-sensing to the photogrammetrists. But as the current performance of the hardware is inadequate, so the discussions regarding the pertinent software may seem rather futuristic. At present, it seems more realistic to think of contouring from a dense net of spot heights measured with an APR and only using the imagery on one hand for the planimetric positioning of the height points and on the other hand for limited secondary height interpolation.

At the present time, even these procedures cannot be expected to reach the precision of contours obtained by conventional photogrammetric methods, but they may well be useful in areas such as those with continuous dense cloud cover where conventional photography cannot be taken.

Acknowledgement

I wish to express my gratitude to all my colleagues who have helped me with this report, especially to Ir. S.A. Hempenius, Mr. G. Petrie, Dr. P. Stefanovič and Mr. G. Gustafson.

I thank Prof. Dr. H.G. Jerie for the opportunity to undertake this study.

REFERENCES :

[0] Anonymous "Voorstel tot Applikatie Onderzoek van Moderne Lucht-opname Technieken", ITC, January 1969.

[1] Anonymous "Bendix Thermal Mapper", Techn. Inf., Bendix Aerospace Systems Division.

[2] Anonymous "Side Looking Radar Used", World Oil, Jan. 1970, p. 4.

[3] Crandall, C.J. "Radar Mapping in Panama", Photogrammetric Engineering, Vol. XXXV, No. 7, 1969, p. 641-646.

[4] Eppler, W.G. & Derrill, R.D. "Relating Remote-Sensor Signals to Ground Truth Information", Proc. IEEE, Vol. 57, No. 4, 1969, p. 665-675.

[5] Hempenius, S.A. "Image Formation Technique for Remote-Sensing from a Moving Platform", ITC-Publ., Series A, No. 46, 1969.

[6] Hempenius, S.A. "The Role of Image Quality in Photogrammetric Pointing Accuracy", Final Tech. Report, European Research Office, United States Army, Contract No. DA-91-591-EUC-3721, 1969.

[7] Konecny, G. & Derenyi, E.E. "Geometrical Considerations for Mapping from Scan-Imagery", Proc. Symp. Remote Sensing Environment, 4th, Ann Arbor, 1966, p. 327-338.

[8] La Prade, G.L. "An Analytical and Experimental Study of Stereo for Radar", Photogrammetric Engineering, Vol. XXIX, No. 2, 1963, p. 294-300.

[9] La Prade, G.L. "Subjective Considerations for Stereo Radar" Paper presented at the ASP-Convention, March 1970, Wash., D.C.

[10] Leberl, F. "Instrumentelle Entzerrung von SLAR- und IRLS-Abbildungen - Beschreibung und Vergleich von Möglichkeiten", Paper presented at the Symp. Comm. II of ISP, Munich, 1970.

[11] Loor, G.P. de — "Possibilities and Uses of Radar and Thermal Infrared Systems", Photogrammetria, Vol. 24, 1969, p. 43-58.

[12] Loor, G.P. de — Personal Communication.

[13] Nims, A.A., — "All Weather Mapping by Radar", Westinghouse Engineer, 1968.

[14] Manual of Photogrammetry — "Photogrammetric & Radargrammetric Techniques", 3rd ed. 1966, chap. XXI.

[15] Moore, R.K., — Univ. of Kansas, Lawrence, Personal Communication.

[16] Ondrejka, R.J. — "Scan-Generated Images for Photogrammetric Tasks", MSc-Thesis, ITC, 1963.

[17] Ramsayer, K. & Tautenhahn, P., — "Ermittlung der zufälligen Messfehler von Grund und Eigengeschwindigkeit, Abtrift und Kurs eines Flugzeuges", Inst. für Flugnavigation, Techn. Univ. Stuttgart, 1965.

[18] Revillon, G., — "Radar à Faiscau Latéral Utilisant une Antenne Synthétique", Paper presented at the 13th Symp. AGARD Avionics Panel, Milan, 1967.

[19] Rosenfield, G.H., — "Stereo Radar Techniques", Photogrammetric Engineering, Vol. XXXIV, No. 6, 1968, p. 587-594.

[20] Yorithomo, K.T., — "Comparison of Photogrammetric and Radar Data Reduction", Techn. Mem., USAETL, Fort Belvoir, USA.

Appendix

A.I. Image Displacement due to the Basic Geometrical Characteristics of the SLAR System

See figure 12:

$k.\Delta y = s - G$ $\qquad$ k ..... scale factor

$G = \rho . R$

$$\cos\rho = \frac{(R+H)^2 + (R+\Delta h)^2 - s^2}{2(R+H)(R+\Delta h)} \approx 1 - \frac{\rho^2}{2}$$

$$\rho^2 \approx \frac{2(R+H)(R+\Delta h) - (R+H)^2 - (R+\Delta h)^2 + s^2}{(R+H)(R+\Delta h)} = \frac{s^2 - (H-\Delta h)^2}{(R+H)(R+\Delta h)}$$

$$G = R.\rho = R\frac{s^2-(H-\Delta h)^2}{(R+H)(R+\Delta h)})^{\frac{1}{2}} = (s^2-(H-\Delta h)^2)^{\frac{1}{2}}(1 + \frac{H+\Delta h}{R} + \frac{H.\Delta h}{R^2})^{-\frac{1}{2}}$$

$$= (s^2-(H-\Delta h)^2)^{\frac{1}{2}}(1 - \frac{H+\Delta h}{2R} + \ldots\ldots)$$

$$G_o^2 = s^2 - H^2$$

$$k.\Delta y \approx s - G_o(1 - \frac{\Delta h^2 - 2H\Delta h}{G_o^2})^{\frac{1}{2}}(1 - \frac{H+\Delta h}{2R} + \ldots\ldots)$$

$$s - G_o(1 - \frac{\Delta h^2 - 2H\Delta h}{2G_o^2} + \ldots\ldots)(1 - \frac{H+\Delta h}{2R} + \ldots\ldots)$$

$$\boxed{k.\Delta y \approx s - G_o + \frac{\Delta h^2 - 2H\Delta h}{2G_o} + \frac{G_o H}{2R} + \frac{2G_o^2 - (H+\Delta h)(\Delta h - 2H)\Delta h}{4G_o R}}$$

A.2. Image Displacement due to an Erroneous Exterior Orientation of the SLAR System

dbx:

$$\boxed{\begin{array}{l} k.\Delta x = -dbx \\ k.\Delta y = o \end{array}}$$

dby:

$s = (H^2 + G_o^2)^{\frac{1}{2}}$ $\qquad$ $ds = k.\Delta y$

$ds = (H^2 + G_o^2)^{-\frac{1}{2}} . G_o . dG_o$ $\qquad$ $dG_o = -dby$

$$\boxed{\begin{array}{l} k.\Delta x = o \\ k.\Delta y = (-G_o/s)dby \end{array}}$$

Appendix

dbz:

$s = (H^2+G_o^2)^{\frac{1}{2}}$

$ds = k.\Delta y = (H/s)dH \qquad dH = dbz$

$$\boxed{\begin{aligned} k.\Delta x &= o \\ k.\Delta y &= (H/s)dbz \end{aligned}}$$

$d\kappa$:

$ds = (G_o/s)dG_o \qquad dG_o = G_o(1-\cos d\kappa) = G_o(d\kappa^2/2)$

$$\boxed{\begin{aligned} k.\Delta x &= G_o d\kappa \\ k.\Delta y &= (G_o^2/2s)d\kappa^2 \end{aligned}}$$

$d\varphi$:

$$\boxed{\begin{aligned} k.\Delta x &= H.d\varphi \\ k.\Delta y &= o \end{aligned}}$$

B.1. Image Displacement due to the Basic Geometrical Characteristics of the IRLS System

See figure 12:

$k.\Delta y = H.A - R.\rho$

$$\sin(\rho+A) = \sin A.\frac{R+H}{R+\Delta h}$$

$$\rho = \underbrace{\arcsin(\sin A.\frac{R+H}{R+\Delta h})}_{C} - A$$

Developing $\frac{R+H}{R+\Delta h}$ in a series gives:

$$C = \arcsin(\sin A(1+\frac{H}{R})(1-\frac{\Delta h}{R}+\ldots\ldots)$$

$$C = \arcsin(\sin A + \sin A(\frac{H}{R}-\frac{\Delta h}{R}+\frac{\Delta h^2}{R^2}-\frac{\Delta h.H}{R^2}+\ldots\ldots))$$

Considering sinA as the independent variable and $\sin A(\frac{H}{R}-\frac{\Delta h}{R}+\ldots\ldots)$ as its finite increment, development of C in a series gives:

$$C = \arcsin(\sin A) + \frac{\sin A}{\cos A}(\frac{H}{R}-\frac{\Delta h}{R}+\frac{\Delta h^2}{R^2}-\frac{\Delta h.H}{R^2}+\ldots\ldots)+\frac{\sin^3 A}{2\cos^3 A}(\frac{H}{R}-\frac{\Delta h}{R}+\ldots\ldots)^2+\ldots\ldots$$

Neglecting terms of higher order results in:

$$C \approx A + \tan A\left(\frac{H}{R} - \frac{\Delta h}{R} + \frac{\Delta h^2}{R^2} - \frac{\Delta h.H}{R^2}\right) + \frac{\tan^3 A}{2}\left(\frac{H^2}{R^2} + \frac{\Delta h^2}{R^2} + \frac{2\,\Delta h.H}{R^2}\right)$$

Substitution in the original equation gives:

$$k.\,\Delta y \approx H(A - \tan A) + \Delta h.\tan A - \frac{\tan^3 A.H^2}{2R} + \tan A\,\frac{\Delta h}{R}\,(H - \Delta h + \frac{\tan^2 A}{2}\,.\,(2H - \Delta h))$$

B. 2. Image Displacement due to an Erroneous Exterior Orientation of the IRLS System

dbx:

$$k.\,\Delta x = -dbx$$
$$k.\,\Delta y = o$$

dby:

$$A = \arctan(G_o/H)$$
$$dA = (\cos^2 A/H)\,dG_o \qquad dG_o = -dby$$

$$k.\,\Delta x = o$$
$$k.\,\Delta y = -\cos^2 A.\,dby$$

dbz :

$$dA = -(\sin(2A)/2).\,dbz$$

$$k.\,\Delta x = o$$
$$k.\,\Delta y = -\frac{\sin 2A}{2}\,dbz$$

$d\varphi$:

$$k.\,\Delta x = H.\,d\varphi$$
$$k.\,\Delta y = o$$

$d\omega$:

$$k.\,\Delta x = o$$
$$k.\,\Delta y = -H.\,d\omega$$

$d\kappa$:

$$dA = \frac{\cos^2 A}{H}\,dG_o = \frac{\cos^2 A}{H}\,G_o\,(\frac{1-\cos d\kappa}{\cos d\kappa}) = \frac{\cos^2 A}{H.2}\tan A.\,H.\,d\kappa^{\,2}$$

$$k.\,\Delta x = \tan A.\,H.\,d\kappa$$
$$k.\,\Delta y = \frac{H.\sin(2A)}{4}\,d\kappa^{\,2}$$